

Preparation of Electrospun Oxidized Cellulose Mats and Their *in vitro* Degradation Behavior

Myung Seob Khil, Hak Yong Kim*, Young Sic Kang, Ho Ju Bang, and Douk Rae Lee

Department of Textile Engineering, Chonbuk National University, 664-14 Dukjin, Dukjin, Chonju, Chonbuk 561-756, Korea

Jae Kyun Doo

Department of General Gynecology and Obstetrics med. School, Chonbuk National University, 664-14 Dukjin, Dukjin, Chonju, Chonbuk 561-756, Korea

Received November 5, 2004; Revised January 17, 2005

Abstract: This paper investigated the effect of biodegradation behavior on the oxidation of cellulose nanofiber mats. The cellulose mats were produced through electrospinning. The diameter of an electrospun fiber varied from 90 to 240 nm depending on the electrospinning parameters, such as the solution concentration, needle diameter, and rotation speed of a grounded collector. Oxidized cellulose (OC) mats containing different carboxyl contents were prepared using NO₂ as an oxidant. The total carboxyl content of the cellulose nanofiber mats obtained after oxidation for 20 h was 20.6%. The corresponding carboxyl content was important from a commercial point of view because OC containing 16-24% carboxyl content are used widely in the medical field as a form of powder or knitted fabric. Degradation tests of the OC mats were performed at 37 °C in phosphate-buffered saline (pH 7.4). Microscopy techniques were introduced to study the morphological properties and the degradation behavior of the OC mats. Morphological changes of the mats were visualized using optical microscopy. Within 4 days of exposure to PBS, the weight loss of the OC mats was >90%.

Keywords: electrospun oxidized cellulose mats, electrospinning, carboxyl content, swelling, degradation behavior.

Introduction

Electrospinning^{1,2} is receiving increasing attention because it can permit an attractive approach to the fabrication of fibrous biomaterials for a variety of applications, including tissue engineering,³⁻⁵ vascular grafts,⁶ tissue repair,⁷ wound healing,⁸ and drug delivery.⁹ The most representative characteristic is to generate very fine fibers (generally down to ca. 50 nm diameters), which lead to several desirable characteristics such as relatively large surface area to volume ratio, flexibility in surface modification, and superior mechanical performance compared with any other known forms. The origin of electrospinning dates back more than 70 years. Since Formhals¹⁰ published a series of patents, many researchers have reported that nearly hundreds of different polymers have been successfully spun into ultrafine fibers using this technique.¹¹ Owing to their efforts, interest of the electrospinning process has been steadily extended especially in industrial fields recently. For example, the best rep-

resentatives appear in the field of filtration systems¹² and medical prostheses mainly focusing on grafts and vessels.¹³

Most of the human tissues and organs are recognized as nanofibrous forms or structures. As such, current research in electrospun nanofibers has focused one of their major applications on bioengineering and promising potential has been found in various biomedical areas. For example, electrospun biocompatible polymer nanofibers have been fabricated as thin porous film designed to be implanted into human body for the replacement of hard tissues.¹⁴⁻¹⁶

To be used as a biomaterial for successful implantation, a polymer must be biodegradable and biocompatible¹⁷ and must contain appropriate functional sites for modification¹⁸ of its degradation property. Moreover, the polymer and its degradation products must be non-immunogenic, non-toxic, and effectively metabolized from the body.

It is well known that cellulose and its derivatives have a good biocompatibility.¹⁹⁻²⁵ Oxidized cellulose (OC) (Figure 1) with carboxyl groups is an especially important class of biodegradable polymers. Oxidized polymer with 16-24% of carboxyl content is widely used in medical areas²⁶⁻²⁸ in powder or knitted fabric form, which can stop bleeding during

*e-mail: khy@chonbuk.ac.kr, m-skhil@hanmail.net
1598-5032/02/62-06©2005 Polymer Society of Korea

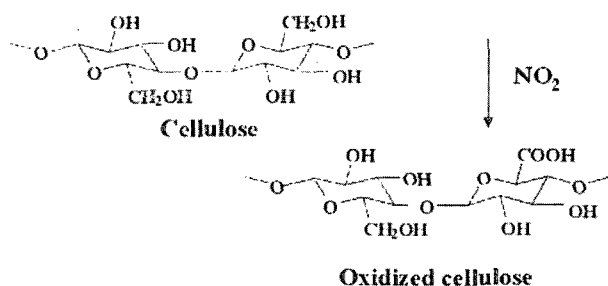


Figure 1. Pathway for oxidation of electrospun cellulose mats.

surgery and prevent the formation/reformation of post-surgical adhesions.

In this study, cellulose mats were first prepared via electrospinning to understand the link between spinning parameter and fiber morphology. Electrospun cellulose mats were subsequently oxidized by nitrogen dioxide (NO₂). In order to investigate the influence of carboxyl content on degradation behavior, the degradation of electrospun OC mats was performed using phosphate buffered saline (pH 7.4) at 37 °C for a predetermined period of time. OC was chosen as a model electrospun polymer for several reasons, namely, it is applicable to various medical areas, is well established, and possesses excellent biocompatibility. The incorporation of carboxyl acid into electrospun cellulose mats was performed to accelerate degradation. This paper will present how to prepare oxidized electrospun cellulose mat and discuss morphological characteristics as well as degradation behavior of the electrospun cellulose mats after exposure to phosphate buffered saline.

Experimental

Materials. Cellulose (DP-670 grade) was obtained from ITT-Rayonier Inc. *N*-methylmorpholine-*N*-oxide (NMMO) with 50% H₂O, the only direct solvent²⁹ used industrially, was obtained from BASF. Solutions of cellulose and NMMO (50% H₂O) with compositions ranging from 2 to 9% (w/v) were prepared using rotary evaporator at around 80 °C under vacuum until complete dissolution of polymer occurred. Solutions for electrospinning were then cooled to room temperature.

Electrospinning. The apparatus used in the electrospinning process is shown in Figure 2. It consists of a syringe and capillary tip with variable diameter, a ground electrode, and high voltage power supply (CPS-60 k02v1, Chungpa EMT Co., South Korea).

Polymer solution was continuously supplied from a syringe using micro tube pump (MP-3N, Tokyo Rikakikai Co. Ltd., Japan). The syringe used in these experiments has interchangeable capillary tips with diameters ranging from 0.3 to 1.1 mm. The electric field was provided by a high voltage power supply that can generate voltage of up to 50 kV. The

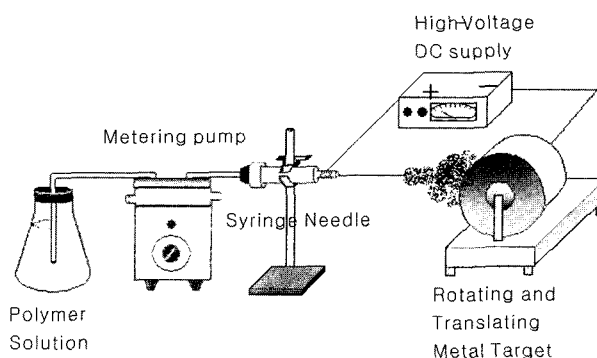


Figure 2. Schematic representation of the electrospinning set-up. An electric field is generated by applying a high voltage between the needle and collector. The volumetric feed rate is controlled through the use of the metering pump. Rotating drum can be controlled to have a speed ranging from 0 to 5.5m/s.

copper probe of the generator was connected with the syringe needle and electricity was conducted through the solution. A grounded rotating drum that deposited the fibers was positioned horizontally from the needle of the syringe. The resulting fibers were collected on a metal drum that has a rotation speed of collector ranging from 0.4 to 1.6 ms⁻¹, to produce a sheet of nonwoven fabric.

Preparation of OC Mats. Nitrogen dioxide (NO₂), NaOH, and 2-propanol were purchased from Aldrich and used as received. FC-84, a perfluorocarbon available from 3M Company, and nitrogen dioxide were mixed in 3:1 (v/v) ratio.³⁰ To a 60 mL mixture, 5 g of electrospun cellulose was added. Reaction time varied from 0 to 20 h and reaction temperature was kept at 25 °C, with constant stirring using a perforated mandrel. OC mats obtained were rinsed with a mixture of 2-propanol/water (50/50, v/v) and, in turn, the residual mixture on the electrospun cellulose mats was neutralized by adding 1% NaOH. The resultant product was washed with 2-propanol several times to wash out the excess NO₂. The modified materials were then dried in air at room temperature.

Fourier-transform Infrared (FT-IR). The FT-IR spectra of samples were obtained from films with a Nicolet Magna-IR 560 spectrophotometer.

Determination of Carboxyl Content. The quantification of free carboxyl content in the sample was determined by a method from the United States Pharmacopoeia (USP, 1995). Approximately 0.5 g of the sample was accurately weighed and suspended in 50 mL of a 2% (w/w) calcium acetate solution for 30 min. The mixture was titrated with standardized 0.1 N NaOH solution using phenolphthalein, as an indicator, until a pink color was obtained. The volume of NaOH solution consumed was corrected for the blank. The carboxyl content in the sample was calculated using the following equation:

$$\text{Carboxyl content (\%, w/w)} = \frac{N \times V \times M_{w\text{COOH}}}{\text{Weight of sample (mg)}} \quad (1)$$

Where N is the normality of NaOH, and V is the volume of NaOH in mL consumed in titration, after correcting for the blank.

***In vitro* Degradation of Electrospun OC Mats.** The electrospun OC mats with a size of 2×10 cm were transferred to a screw-top vial. To each vial, 20 mL of phosphate buffered saline (pH 7.4) was added using a pipette. The vials were moved in a shaking water bath, maintained at 37°C , at constant agitation ($60 \text{ shakes min}^{-1}$). At predetermined time intervals, the sample vials were removed from the shaking water bath and thermal stabilities of the sample were measured by thermogravimetric analyzer (Perkin-Elmer TGA-7) at a heating rate of 10°C/min under nitrogen atmosphere.

Measurements and Characterization. The mass loss was calculated by comparing the dry weight (m_f) remaining at a given hydrolysis with the initial weight (m_i) according to the equation:

$$\% \text{ mass loss} = \frac{(m_i - m_f)}{m_i} \times 100 \quad (2)$$

Optical micrographs were taken with a Nikon Eclipse ME600 model to investigate degradation behavior of mats as a function of immersion time.

Results and Discussion

Cellulose solution was dissolved in NMMO with 50% H_2O and the electrospinning parameters were varied. Parameters tested, such as solution concentration, needle diameter, and rotation speed, greatly affected the morphology of cellulose

as shown in Figure 3 (under a voltage of 15 kV). It is well known that a major determinant of fiber morphology is solution concentration. The cellulose solution in NMMO with 50% H_2O could not be electrospun into fibers at concentrations below 4 wt%. The diameter and shape of the fibers appear to be sensitive to needle diameter as well as solution concentration. As the needle diameter is decreased, the diameter of the fibers decreases greatly. However, the differences in morphology of electrospun mats were not significant with increasing of rotation speed of grounded collector. The uniform fibers that have the diameter ranging from 90 to 250 nm were formed using a polymer concentration of 4 wt%, and this concentration was employed for the latter experiments.

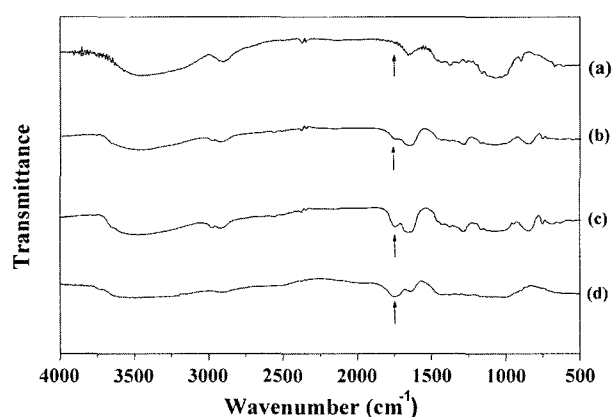


Figure 4. FT-IR spectra of (a) electrospun cellulose mats and electrospun OC mats reacting with NO_2 for (b) 5 h, (c) 10 h, and (d) 20 h.




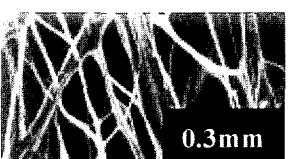

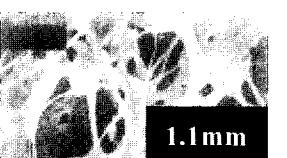
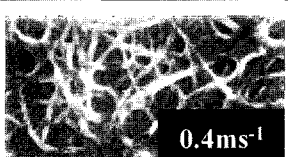
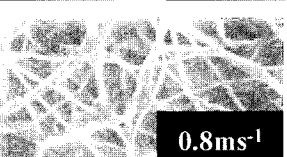
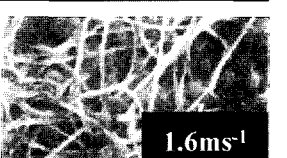
Parameter	Morphological changes		
Solution concentration	 2wt%	 3wt%	 4wt%
Needle diameter	 0.3mm	 0.7mm	 1.1mm
Rotation speed	 0.4ms^{-1}	 0.8ms^{-1}	 1.6ms^{-1}

Figure 3. The effect of process parameters on cellulose morphology. The process parameters of solution concentration, needle diameter, and winding velocity can be combined to produce cellulose nanofiber mats.

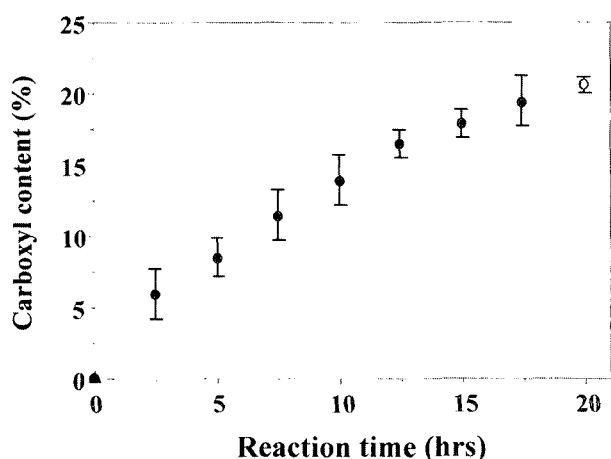


Figure 5. Change in carboxyl content with reaction time for oxidation of electrospun cellulose with NO_2 at 25°C .

The electrospun cellulose mats were examined by FT-IR after they had been oxidized for 5, 10, and 20 h. Figure 4 shows the FT-IR spectrum in the spectral range $500\text{--}4000\text{ cm}^{-1}$, which was in excellent agreement with those reported in the literature,³¹ for a cellulose sample before and after oxidation. The characteristic carboxyl absorption peak at 1745 cm^{-1} ($\nu_{\text{C=O}}$), which was noted for OC, increased with increasing reaction time.

The effect of reaction duration on the carboxyl content of OC mats is shown in Figure 5. The carboxyl content in the products increased when reaction time was increased from 2.5 to 20 h. The total carboxyl content of the OC mats obtained after 20 h was 20.6%. OC containing 16–24% carboxyl content is commercially available in various forms because the corresponding carboxyl content shows proper biodegradability for use in human. Therefore, the carboxyl content of electrospun OC mats prepared from this study is sufficient to allow for the necessary biodegradability.

Figure 6 shows TGA curves of electrospun cellulose mats oxidized by NO_2 in each reaction time. Initial weight loss which is attribute to loss of water increased as reaction time increased. This is consistent with the results shown in Figures 4 and 5. It can be explained that the affinity of the material on water molecules increases as the carboxyl content increases. As expected, the thermal stability of OC mats decreased as the carboxyl content increased. The initial degradation of electrospun OC mats for 20 h of reaction time (carboxyl content ca. 20.6%) was 186°C .

When electrospun OC mats contacted with the buffer solution at 37°C , weight loss occurred rapidly. These results of electrospun OC mats are shown in Figure 7. The results reveal that all samples lost their mass almost linearly with immersion time, except electrospun OC mats for 5 h of reaction time, but their degradation rate slowed down with decreasing reaction time. The linear rate of mass loss observed in this study strongly suggests that the degraded

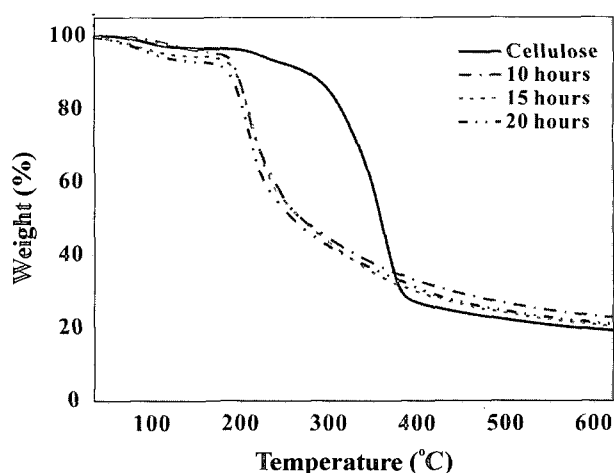


Figure 6. TGA traces of untreated and NO_2 oxidized electrospun cellulose mats with different reaction times.

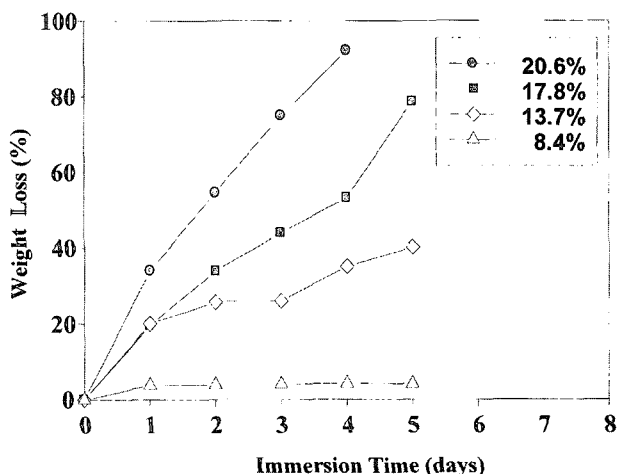


Figure 7. *In vitro* degradation of electrospun OC mats with different carboxyl content. *In vitro* degradation of electrospun OC mats is represented as a function of weight loss over immersion time.

samples can easily reach the media, which means that these mats contain many channels that allow the degradation products to leave the bulk polymer mats immediately when formed. It seems that sufficient swelling of each nanofiber helps give a better chance for water to make contact with the electrospun OC mats from the beginning of the hydrolysis experiment.

To examine the morphological change of electrospun OC mats after exposure to buffer solution, light microscopy were introduced. Figure 8 shows light photomicrographs of electrospun OC mats with 20.6% carboxyl content after different degradation periods. Morphological change was noticed on electrospun OC mats at 2 days after exposure to buffer solution. As degradation advanced, the nanofibrous structure

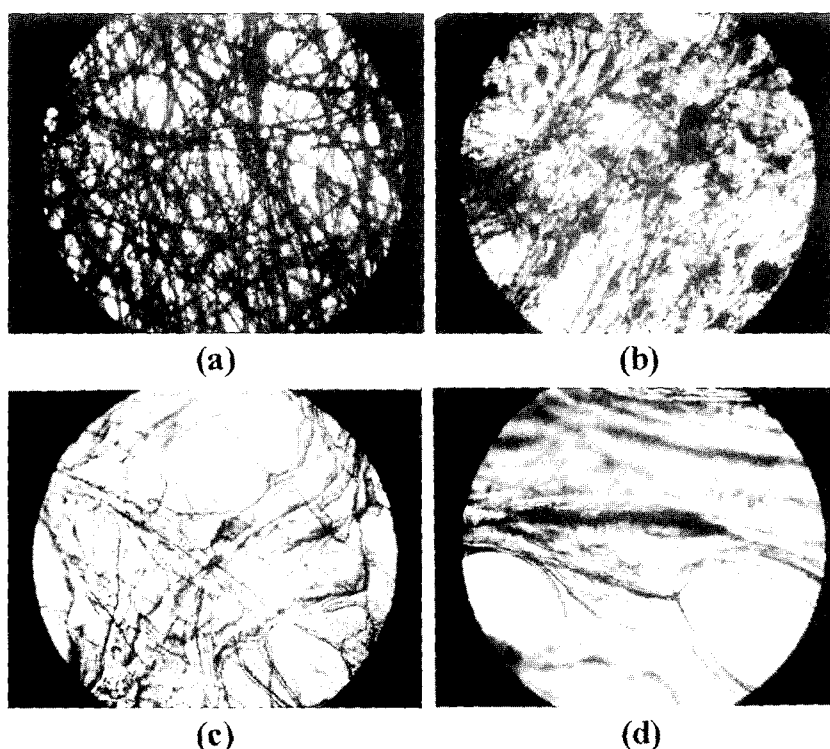


Figure 8. Optical photographs of electrospun OC mats with (a) 1 day, (b) 2 days, (c) 3 days, and (d) 4 days of immersion time in PBS (pH 7.4) at 37 °C, respectively. The carboxyl content of electrospun OC mats is 20.6% ($\times 500$).

could no longer be observed as shown in Figure 8(c) and (d). These results strongly suggest that the mass loss is probably due to combination of two factors. The rapid degradation of electrospun OC mat results from higher surface areas and porous structure. Also, these photographs clearly indicate the time-dependent degradation behavior of electrospun OC nanofiber mats.

Conclusions

Nanofiber cellulose mats, with diameters ranging from 90 to 250 nm, were prepared via electrospinning and the resultant mats were successfully oxidized by NO_2 . When the electrospun cellulose mats were oxidized with NO_2 , the total carboxyl content of the OC mats obtained after 20 h was 20.6%. The affinity of the material for water molecules increased as the carboxyl content of OC mats increases, whereas the thermal stability of the OC mats decreased as the carboxyl content increases. The degradation test revealed that all the samples lost their mass almost linearly with reaction time, but their degradation rate slowed down as reaction time decreases. The linear rate of mass loss observed in this study strongly suggests that the degraded samples can easily make contact with the media, which means that these samples contain many channels, and degradation products leave the bulk polymer mats immediately when formed. As degrada-

tion advanced, the nanofibrous structure was not observed any more. In conclusion, the electrospun OC mats is more likely exposed to the surface and much less diffusional resistance can be expected because of their higher surface areas and porous structure.

Acknowledgements. The authors thank the Korean Ministry of Science and Technology for financial support through the Center for Healthcare Technology Development.

References

- (1) D. H. Reneker and I. Chun, *Nanotechnology*, **7**, 216 (1996).
- (2) J. M. Deitzel, W. Kosik, S. H. McKnight, N. C. B. Ten, J. M. Desimone, and S. Crette, *Polymer*, **43**, 1025 (2002).
- (3) C. J. Buchko, L. C. Chen, Y. Shen, and D. C. Martin, *Polymer*, **40**, 7397 (1999).
- (4) A. Fertala, W. B. Han, and F. K. Ko, *J. Biomed. Mater. Res.*, **57**, 48 (2001).
- (5) L. Huang, R. A. McMillan, R. P. Apkarian, B. Pourdeyhimi, V. P. Conticello, and E. L. Chaikof, *Macromolecules*, **33**, 2989 (2000).
- (6) J. D. Stitzel, K. Pawlowski, G. E. Wnek, D. G. Simpson, and G. L. Bowlin, *J. Biomater. Appl.*, **15**, 1 (2001).
- (7) E. D. Boland, G. E. Wnek, D. G. Simpson, K. J. Pawlowski, and G. L. Bowlin, *J. Macromol. Sci.*, **38**, 1231 (2001).
- (8) M. S. Khil, D. I. Cha, H. Y. Kim, I. S. Kim, and N. Bhattarai,

- J. Biomed. Mater. Res.*, **67**, 675 (2003).
- (9) E. Zussman, A. L. Yarin, and D. Weihs, *Experiments in Fluids*, **33**, 315 (2002).
- (10) A. Formhals, GB Pat. 364780 (1929).
- (11) Z. M. Huang, Y. Z. Zhang, M. Kotaki, and S. Ramakrishna, *Composites Science and Technology*, **63**, 2223 (2003).
- (12) P. W. Gibson, H. L. Schreuder-Gibson, and D. Rivin, *AIChE J.*, **45**, 190 (1999).
- (13) L. Gary, K. J. Bowlin, and E. D. Pawlowski, in *Tissue Engineering and Biodegradable Equivalents: Scientific and Clinical Application*, K. U. Lewandrowski, L. W. Donald, J. T. Debra, D. G. Joseph, J. Y. Michael, and E. A. David, Eds., Marcel Dekker, New York, 2002, pp 165-78.
- (14) S. A. Athreya and D. C. Martin, *Sensor. Actuat. A-Phys.*, **72**, 203 (1999).
- (15) C. J. Buchko, M. J. Slattey, K. M. Kozloff, and D. C. Martin, *J. Mat. Res.*, **15**, 231 (2000).
- (16) C. J. Buchko, K. M. Kozloff, and D. C. Martin, *Biomaterials*, **22**, 1289 (2001).
- (17) J. C. Pommier, J. Poustis, C. Baquey, and D. Chauveaux, Fr. Pat. 8610331 (1986); Eur. Pat. 0256906 A1 (1987); U. S. Pat. 4904258 (1990).
- (18) P. L. Granja, M. A. Barbosa, L. Pouységu, B. De Jésus, and C. Baquey, in *Frontiers in Biomedical Polymers Applications 2*, R. Ottenbrite, Ed., Technomic Press, Lancaster, PA, USA, 1999, pp 195-225.
- (19) M. Martson, J. Viljanto, T. Hurme, and P. Saukko, *Eur. Surg. Res.*, **30**, 426 (1998).
- (20) U. Gross, C. Muller-Mai, and C. Voigt, *Fourth World Biomaterials Congress*, April, Berlin, Germany, 1992, p. 192.
- (21) D. Chauveaux, C. Barbie, X. Barthe, C. Baquey, and J. Poustis, *Clin. Mater.*, **5**, 251 (1990).
- (22) Y. Ikada, in *Cellulose: Structural and Functional Aspects*, J. F. Kennedy, G. O. Phillips, and P. A. Williams, Eds., Ellis Horwood, Chichester, UK, 1989, pp 447-455.
- (23) T. Miyamoto, S. Takahashi, H. Ito, H. Inagaki, and Y. Noishiki, *J. Biomed. Mater. Res.*, **23**, 125 (1989).
- (24) G. Franz, *Adv. Polym. Sci.*, **76**, 1 (1986).
- (25) B. Philipp, W. Bock, and F. Schierbaum, *J. Polym. Sci. Polym. Symp.*, **66**, 83 (1979).
- (26) G. S. Banker and V. Kumar, U. S. Pat. 5,405,953 (1995).
- (27) D. M. Wiseman, L. Saferstein, and S. Wolf, U. S. Pat. 6,500,777 B1 (2002).
- (28) P. N. Galgut, *Biomaterials*, **11**, 561 (1990).
- (29) T. Röder and B. Morgenstern, *Polymer*, **40**, 4143 (1999).
- (30) B. Franklin and S. Lowell, U. S. Pat. 5,180,398 (1993).
- (31) V. Kumar and T. Yang, *Carbohydrate Polymer*, **48**, 403 (2002).